Design of a Rectal Probe for Diffuse Optical Spectroscopy Imaging for Chemotherapy and Radiotherapy Monitoring

Martijn van de Giessen[1,2], Ylenia Santoro[3], Soroush Mirzaei Zarandi[3], Alessio Pigazzi[4], Albert E. Cerussi[3], Bruce J. Tromberg[3]
[1]Division of Image Processing, Leiden University Medical Center, Leiden, The Netherlands;
[2]Department of Intelligent Systems, Delft University of Technology, Delft, The Netherlands;
[3]Beckman Laser Institute, University of California Irvine, Irvine CA, United States of America;
[4]Division of Colorectal Surgery, School of Medicine, University of California Irvine, Irvine CA, United States of America.

ABSTRACT

Diffuse optical spectroscopy imaging (DOSI) has shown great potential for the early detection of non-responding tumors during neoadjuvant chemotherapy in breast cancer, already one day after therapy starts. Patients with rectal cancer receive similar chemotherapy treatment. The rectum geometry and tissue properties of healthy and tumor tissue in the rectum and the requirement of surface contact impose constraints on the probe design.

In this work we present the design of a DOSI probe with the aim of early chemotherapy/radiotherapy effectiveness detection in rectal tumors. We show using Monte Carlo simulations and phantom measurements that the colon tissue can be characterized reliably using a source-detector separation in the order of 10 mm. We present a design and rapid prototype of a probe for DOSI measurements that can be mounted on a standard laparoscope and that fits through a standard rectoscope. Using predominantly clinically approved components we aim at fast clinical translation.

1. INTRODUCTION

Rectal cancer is characterized by a low 5-year survival rate, until recently even lower than 50% [1]. To increase survival, different therapies are combined, typically chemotherapy and radiation therapy, often followed by surgery. However, chemotherapy and radiation often (up to 30%) do not reach a pathologically complete response (no vital tumor cells left) or some patients do not respond at all, particularly to chemotherapy. These response variations require the monitoring of tumor response during therapy.

To measure the tumor response in early therapy stages, functional imaging, e.g. of tumor metabolism changes, is preferred over structural imaging which only measures secondary therapy effects. Apart from nuclear modalities, perfusion based magnetic resonance imaging (MRI) and computed X-ray tomography have been used for functional tumor imaging. All these methods, however, have drawbacks that prevent frequent monitoring, particularly injections of radiotracers or contrast agents and/or ionizing radiation.

Diffuse optical spectroscopy is a promising modality that does not suffer from these drawbacks. Here, inherent optical tissue contrast is used to, typically, measure blood content and oxygenation as well as water and lipid concentrations [2-4]. By measuring in the near-infrared (NIR), tissue optical properties can be determined up to a few centimeters deep. In chemotherapy monitoring of the breast this modality has shown promising results [3, 5]. Particularly promising is Diffuse Optical Spectroscopy Imaging [4], which has shown in pilot studies to allow tumor response prediction already one day after the start of chemotherapy [6]. However, diffuse optical spectroscopy measurements require the measurement probe to touch the tissue under investigation to prevent light reflections at the air-tissue boundary. When measuring tumors close to the outside skin (as in breast), probe size and geometry are relatively unrestricted. Measuring in the rectum poses additional geometric and accessibility challenges:

Endoscopic Microscopy IX; and Optical Techniques in Pulmonary Medicine, edited by Guillermo J. Tearney, Thomas D. Wang, Melissa J. Suter, Stephen Lam, Matthew Brenner, Proc. of SPIE Vol. 8927, 89270G

1. Measurements have to take place in a confined space. This limits the probe size and thereby also significantly changes measurement characteristics.

2. The colon wall is relatively thin (~2.5 mm) compared to the penetration depth of NIR light. The properties of deeper tissue are uncertain and may vary, thereby increasing measurement uncertainty.

3. No direct vision is available for the operator. This complicates measuring at the correct location and with good tissue contact.

4. The probe should be safe for internal use and easy to clean.

These challenges have been partly addressed in [7], but the short distances between source and detector fibers (0-4 mm), restrict measurements to (close to) the tissue surface.

In this work we perform a feasibility study to the application of diffuse optical spectroscopy imaging (DOSI) in the rectum. We address the challenges above by designing a rectum probe that can be mounted on a standard 10 mm diameter laparoscope. Expected measurement results are simulated using Monte Carlo simulations and the feasibility of measuring using a small probe is validated with phantom measurements.

2. METHODS

2.1 Diffuse optical spectroscopy imaging

Important parameters that influence the trajectories of photons in tissue are the refractive index of the tissue n, the reduced scattering coefficient μs' and the absorption coefficient μa. While n can be considered constant (typically in the order of n=1.4), large variations exist in μs' and μa between different biological tissues. The coefficients μs' and μa are wavelength dependent and provide intrinsic tissue contrast (Figure 2).

DOSI uses intensity modulated laser diodes and NIR broadband illumination to separate the μs' and μa in the complete NIR range, between 650 and 1000 nm [5, 8] (Figure 1). Source and detector fibers are spatially separated, at a distance ρ. Depending on the modulation frequency, μs' and μa and ρ, the detected intensity signal is attenuated and phase-shifted with respect to the illumination source. As the modulation frequency is known, μ_s' and μ_a can be solved for (See details in [8]). In strongly scattering media ($\mu_s' >> \mu_a$) such as biological tissue and for large source-detector separations ($\rho >> 1/(\mu_s' + \mu_a)$), the diffusion approximation can be used. In this work four intensity modulated laser diodes (660, 690, 785, 830 nm) are used which perform a frequency sweep between 0 and 500 MHz. The modulated signal is detected using an avalanche photo diode (APD). Wide near-infrared spectral measurements as in Figure 2 are obtained from a halogen lamp, which response is measured using a spectrometer. From this broadband signal, the scatter and absorption coefficients along the complete spectrum between 650 nm and 1000 nm are estimated by calibrating this signal using the scatter and absorption estimates at the 4 modulated wavelengths (See details in [8]).

2.2 Expected colon tissue optical properties

Healthy colon tissue consists of a layered structure with varying optical properties. As we are currently unable to measure these properties using DOSI, we have to rely on literature for scattering and absorption estimates. In the scarce literature available with in-vivo colon measurements, Zonios, et al. [9] mainly report measurements of the superficial epithelial layer. Hidović-Rowe and Claridge [10] use in-vitro measurements of absorber concentrations and wavelength independent scattering properties (scatter size, volume fraction) to determine the absorption and

scattering within the visible range and validate these in-vivo. Further literature, e.g. [11] report in-vitro measurements without in-vivo validation.

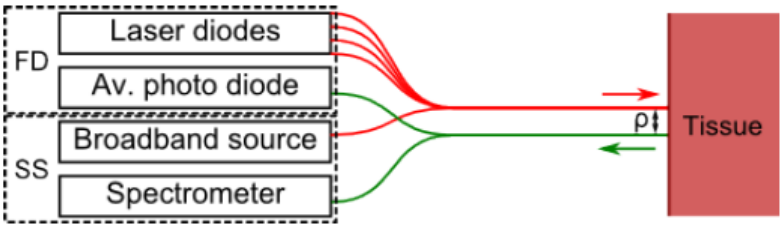

Figure 1: Schematic representation of the DOSI measurement setup combining the frequency domain (FD) and broadband steady state (SS) acquisition. The positions of the (red) source fiber and the (green) detector fiber on the tissue are separated by a distance ρ.

The wavelength independent absorber and scattering properties of the healthy colon layers in [10] allow us to compute the expected absorption and reduced scattering coefficients in the near-infrared region (650-1000 nm). In this work we follow their division of the colon in three tissue layers: mucosa, submucosa and muscularis with average thicknesses of 560, 540 and 800 µm, respectively. The absorption and reduced scattering coefficients in Figure 2a,c have been derived from the hemoglobin, oxygenation, water and lipid contents listed in [10] and the reduced scatter coefficients were estimated using Mie theory from reported scatter diameters and refractive indices.

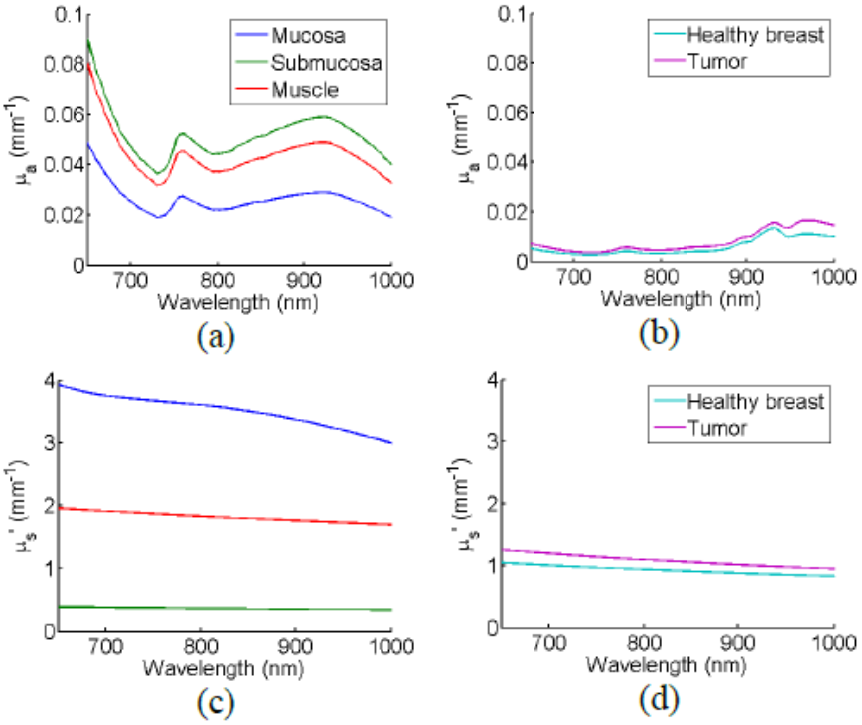

Figure 2: Optical properties for healthy colon and tumor tissue. (a,c) scattering and reduced absorption for healthy colon [10]. (b,d) scattering and reduced absorption for (breast) healthy and tumor tissue [4].

Colon tumor tissue on the other hand does not have a clear layered structure. It starts growing at the inside of the colon wall and expands both into the colon and penetrates towards the outer layers up to thicknesses of

several centimeters. Little information about the optical properties of colon tumor tissue is available from literature. Most work has concentrated on polyp [9] or ex-vivo measurements [11]. Due to lack of in-vivo colon tumor measurements in the near-infrared we will use the optical properties as measured from breast tumor tissue [4], shown in Figure 2b,d.

2.3 Monte Carlo simulations

Frequency domain Monte Carlo simulations [12] were performed to estimate for which source-detector separation distances a sufficiently high phase shift of the modulated signal would be obtained for the separation of scattering and absorption (Section 2.1). To this end the reflectance amplitude and phase were simulated using the tissue properties for both healthy colon and tumor tissue using 10^5 photons.

To investigate which tissue layers in the healthy colon tissue mainly contribute to measured spectra, photon hitting densities (PHD) were estimated by multiplying the fluences of forward and adjoint Monte Carlo simulations [13]. Below the colon tissue layers a 20 mm inter-organ fat layer was added to prevent artifacts due to a tissue-air boundary. Histograms of PHD per tissue layer were computed to estimate the relative contribution of each tissue to the measured signal.

Monte Carlo simulations were performed for wavelengths covering the broadband spectrum: 660, 690, 780, 830, 880, 920, 960, 1000 nm. All layers were assumed to have a limited thickness, but having an infinite extent in the other two dimensions. All simulations were performed using the VirtualPhotonics toolbox (www.virtualphotonics.org).

2.4 Colon phantom

To validate the feasibility of measuring at short source-detector distances in tissues with the properties from Section 2.2, silicon phantoms were created with the properties in Table 1, where μa and μs' are the designed properties at 600 nm. The phantom mimicking healthy colon tissue was made as a homogeneous phantom. Its scatter and absorption coefficients approximated that of a (simulated) layered phantom when measured with a source-detector separation of 10 mm. The latter phantom also contained a 20 mm diameter hole to mimic the inside of the colon. The phantom optical properties were measured using DOSI with $\rho \in \{5,10,13\}$ mm within the phantom cavity and with a multi-distance DOSI probe with source-detector separations at 15, 20, 28 and 35 mm at the phantom surface. The latter measurement counts as the optical properties ground truth.

3. RESULTS

3.1 Monte Carlo: phase shift

Simulated phase shifts at 500 MHz between source signal and detected signal are shown in Figure 3 for healthy colon and tumor tissue. For the target source-detector distance of about 10 mm, phase shifts of about 40-60 degrees can be expected in both tissue types. Given a phase detection precision of about 1 degree with the current fibers, tissue dependent phase shift variations of about 2% can still be detected. For 2.0 mm and 5.0 mm, only phase shifts of 5-40% can be detected, preventing accurate tissue characterization.

Type	SG (ml)	CA (ml)	μ_s' (mm^{-1})	TiO2 (mg)	μ_a (mm^{-1})	Ni (ml)
Healthy	300	30	1.5	0.27	0.025	5.00
Tumor	300	30	1.3	0.35	0.008	0.89

Table 1: Phantom specifications. SG: silicone gel, CA: curing agent, Ni: Nigrosin.

3.2 Monte Carlo: photon hitting densities

Photon hitting densities were computed for 8 wavelengths between 650 nm and 1000 nm for healthy colon and tumor tissue. A typical example at ρ =10 mm for healthy colon at 830 nm is shown in Figure 4a. Although one should note that the visualization uses a logarithmic scale, it is evident that not only the top layers of the colon tissue, but also the auxiliary fat layer contributes significantly to the measured signal at 10 mm source-detector separation. Histograms that show the relative contribution per tissue to the total measured tissue properties are shown in Figure 4b,c,d for a ρ of 5, 10 and 15 mm, respectively. Figure 4c shows that for ρ=10 mm and for most NIR wavelengths almost 50% of the signal comes from the auxiliary fat layer, which is not well defined. Therefore ρ<10 mm is preferable in the rectum. In the thicker tumor tissue (20 mm) practically all signal (>99%) came from the tumor for each simulated ρ and wavelength.

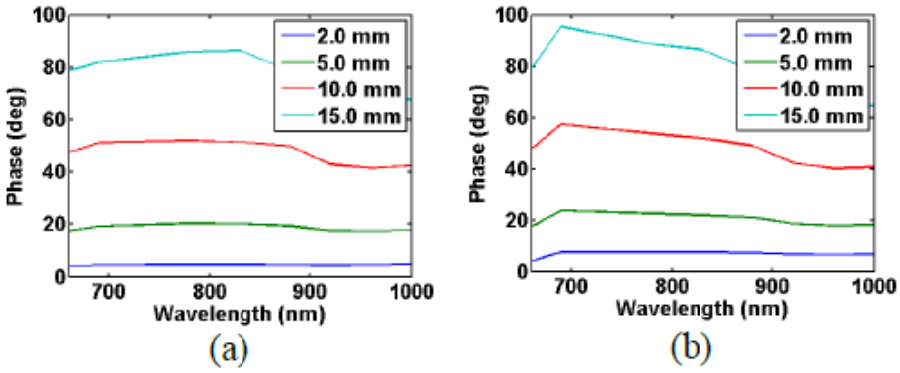

Figure 3: Simulated phase shift as a function of ρ in (a) healthy colon and (b) tumor tissue.

3.3 Phantom measurements

The optical properties of the colon phantom (Figure 6a) were measured 5 times for $\rho \in \{5,10,13\}$ mm in the phantom cavity and with the multi-distance probe on the surface. The averaged estimates for μ_a and μ_s' in the healthy colon phantom are shown in Figure 5. Apart from the source-detector separation at 5 mm, all measured spectra show the same trend. The spectra for 10, 13 mm and the multi-distance probe, do differ, but the small standard deviations show that these measurements are reproducible. Especially the difference between the `10 mm' and `multi' curves show that caution should be taken to compare measurements at different source-detector distances. The deviations at ρ=5 mm are due to small phase shifts and associated almost constant intensity amplitudes over the complete frequency sweep. This prevented accurate model fits and thereby accurate absorption and reduced scattering estimates. At ρ=10 mm absorption and scattering estimates are sufficiently accurate and precise.

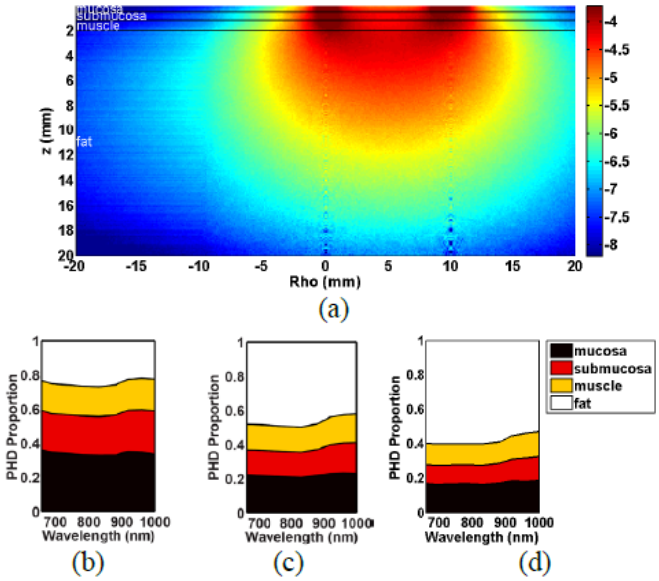

Figure 4: Simulated (a) photon hitting densities in healthy colon at 830 nm for ρ=10 mm. The logarithmic color scale has base 10 and shows normalized data. Wavelength dependent relative photon hitting densities per tissue for ρ's of (b) 5 mm, (c) 10 mm and (d) 15 mm.

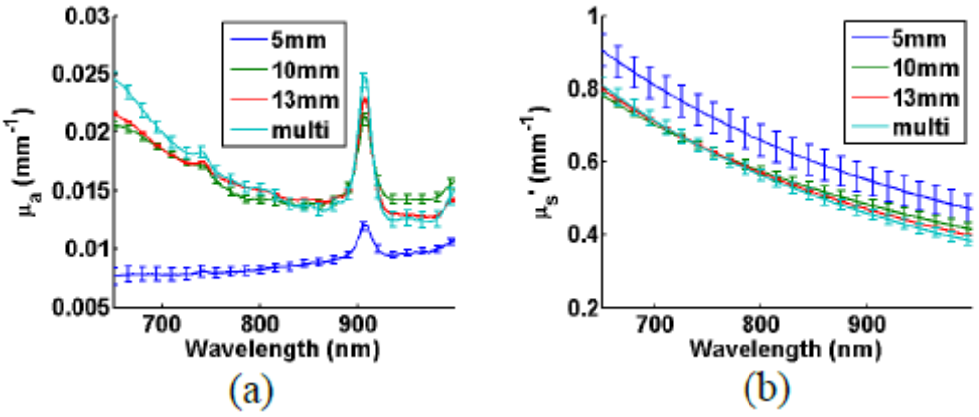

Figure 5: Measurements of (a) absorption and (b) reduced scattering (averaged over 5 measurements) in the healthy colon phantom. Error bars denote standard deviations (shown at coarser sampling).

4. PROBE DESIGN

In Figure 6c,d we present a design with ρ=8 mm that fits through a standard rectum scope of 20 mm outer diameter and 15.5 mm inner diameter. The part guiding the fibers (Figure 6b) can be mounted onto a standard 10 mm diameter laparoscope with a tilted field of view.

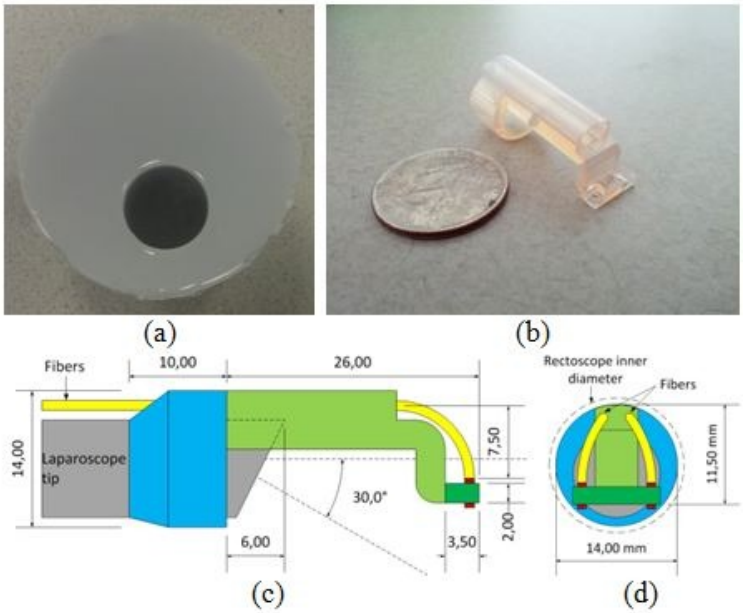

Figure 6: (a) Colon phantom and (b) rapid prototyping fiber guide. Diagram of (c) side- and (d) front-view of rectal probe.

5. DISCUSSION

This feasibility study showed that DOSI measurements are possible within the constraints imposed by the rectum geometry and tissue properties. The Monte Carlo simulations showed that the required short source-detector separations are actually advantageous. Using these short distances, the unknown layer behind the colon muscularis (currently modeled as fat) has a limited contribution to the estimated tissue properties. The phantom experiments showed that measuring at these short distances (~10 mm) is very well feasible. The initial probe design showed that using a standard laparoscope a probe can be devised that fits through the channel of a standard rectum scope. The use of these standard components and the absence of any electric components inside the body significantly simplify clinical translation.

Although not shown explicitly, the used diffusion approximation for photon propagation holds for all of the source-detector distances in this work. However, the tissue properties for healthy colon are an average estimate (See also Section 3.2) that strongly depends on the user-specified source-detector separation.

A limitation of this study is the approximation of colon tumor tissue using breast tumor tissue, probably underestimating absorption. Phantom measurements showed that higher absorption can be measured reliably.

In the near future, the prototype in Figure 6b will be used for pre-clinical in-vivo colon tissue measurements in Yorkshire pigs. Subsequently, this probe will be developed into a clinically applicable device for the early detection of chemotherapy effectiveness and finally a flexible probe will be developed for measuring in the entire colon.

ACKNOLEDGMENTS

This research was supported by the National Center for Research Resources (NCRR, 5P41RR003155) and the National Institute of General Medical Sciences (NIGMS, 8P41GM103540) divisions of the National Institutes of Health (NIH) and the University of California, Irvine (UCI).

REFERENCES

[1] Tepper, J. E., O'Connell, M., Niedzwiecki, D., Hollis, D. R., Benson, A. B., 3rd, Cummings, B., Gunderson, L. L., Macdonald, J. S., Martenson, J. A., and Mayer, R. J., 2002, "Adjuvant therapy in rectal cancer: analysis of stage, sex, and local control--final report of intergroup 0114," Journal of clinical oncology : official journal of the American Society of Clinical Oncology, 20(7), pp. 1744-1750.

[2] Taroni, P., Pifferi, A., Quarto, G., Spinelli, L., Torricelli, A., Abbate, F., Villa, A., Balestreri, N., Menna, S., Cassano, E., and Cubeddu, R., 2010, "Noninvasive assessment of breast cancer risk using time-resolved diffuse optical spectroscopy," J Biomed Opt, 15(6), p. 060501.

[3] Soliman, H., Gunasekara, A., Rycroft, M., Zubovits, J., Dent, R., Spayne, J., Yaffe, M. J., and Czarnota, G. J., 2010, "Functional imaging using diffuse optical spectroscopy of neoadjuvant chemotherapy response in women with locally advanced breast cancer," Clinical cancer research : an official journal of the American Association for Cancer Research, 16(9), pp. 2605-2614.

[4] Cerussi, A., Shah, N., Hsiang, D., Durkin, A., Butler, J., and Tromberg, B. J., 2006, "In vivo absorption, scattering, and physiologic properties of 58 malignant breast tumors determined by broadband diffuse optical spectroscopy," J Biomed Opt, 11(4), p. 044005.

[5] Cerussi, A. E., Tanamai, V. W., Hsiang, D., Butler, J., Mehta, R. S., and Tromberg, B. J., 2011, "Diffuse optical spectroscopic imaging correlates with final pathological response in breast cancer neoadjuvant chemotherapy," Philosophical transactions. Series A, Mathematical, physical, and engineering sciences, 369(1955), pp. 4512-4530.

[6] Roblyer, D., Ueda, S., Cerussi, A., Tanamai, W., Durkin, A., Mehta, R., Hsiang, D., Butler, J. A., McLaren, C., Chen, W. P., and Tromberg, B., 2011, "Optical imaging of breast cancer oxyhemoglobin flare correlates with neoadjuvant chemotherapy response one day after starting treatment," Proc Natl Acad Sci U S A, 108(35), pp. 14626-14631.

[7] Wang, H. W., Jiang, J. K., Lin, C. H., Lin, J. K., Huang, G. J., and Yu, J. S., 2009, "Diffuse reflectance spectroscopy detects increased hemoglobin concentration and decreased oxygenation during colon carcinogenesis from normal to malignant tumors," Opt Express, 17(4), pp. 2805-2817.

[8] Bevilacqua, F., Berger, A. J., Cerussi, A. E., Jakubowski, D., and Tromberg, B. J., 2000, "Broadband absorption spectroscopy in turbid media by combined frequency-domain and steady-state methods," Appl Optics, 39(34), pp. 6498-6507.

[9] Zonios, G., Perelman, L. T., Backman, V., Manoharan, R., Fitzmaurice, M., Van Dam, J., and Feld, M. S., 1999, "Diffuse reflectance spectroscopy of human adenomatous colon polyps in vivo," Appl Opt, 38(31), pp. 6628-6637.

[10] Hidovic-Rowe, D., and Claridge, E., 2005, "Modelling and validation of spectral reflectance for the colon," Phys Med Biol, 50(6), pp. 1071-1093.

[11] Ao, H., Xing, D., Wei, H., Gu, H., Wu, G., and Lu, J., 2008, "Thermal coagulation-induced changes of the optical properties of normal and adenomatous human colon tissues in vitro in the spectral range 400-1,100 nm," Phys Med Biol, 53(8), pp. 2197-2206.

[12] Testorf, M., Osterberg, U., Pogue, B., and Paulsen, K., 1999, "Sampling of time- and frequency-domain signals in monte carlo simulations of photon migration," Appl Opt, 38(1), pp. 236-245.

[13] Hayakawa, C. K., Spanier, J., Bevilacqua, F., Dunn, A. K., You, J. S., Tromberg, B. J., and Venugopalan, V., 2001, "Perturbation Monte Carlo methods to solve inverse photon migration problems in heterogeneous tissues," Opt. Lett., 26(17), pp. 1335-1337.